Biosensors and Bioelectronics 129 (2019) 198–207

Contents lists available at ScienceDirect

Biosensors and Bioelectronics

journal homepage: www.elsevier.com/locate/bios

Saliva-coated titanium biosensor detects specific bacterial adhesion and bactericide caused mass loading upon cell death

Zeqian Xu[a,d], Luisa Coriand[b], Ronny Loeffler[c], Juergen Geis-Gerstorfer[a], Yi Zhou[d], Lutz Scheideler[a], Monika Fleischer[c], Frank K. Gehring[e], Frank Rupp[a,*]

[a] University Hospital Tübingen, Section Medical Materials Science & Technology, Osianderstr. 2-8, D-72076 Tübingen, Germany
[b] Fraunhofer Institute for Applied Optics and Precision Engineering, Albert-Einstein-Strasse 7, D-07745 Jena, Germany
[c] Core Facility LISA+, Eberhard Karls University Tübingen, Auf der Morgenstelle 15, D-72076 Tübingen, Germany
[d] The State Key Laboratory Breeding Base of Basic Science of Stomatology (Hubei-MOST) & Key Laboratory of Oral Biomedicine Ministry of Education, School & Hospital of Stomatology, Wuhan University, 237 Luoyu Road, Wuhan 430079, PR China
[e] 3T analytik, Gartenstrasse 100, D-78532 Tuttlingen, Germany

ARTICLE INFO

Keywords:
Saliva-coated biosensor
QCM-D
Chlorhexidine
Cetylpyridinium chloride
Antibacterial
Cellular leakage

ABSTRACT

Bacteria adhering to implanted medical devices can cause invasive microbial infections, of e.g. skin, lung or blood. In dentistry, *Streptococcus gordonii* is an early oral colonizer initiating dental biofilm formation and also being involved in life-threatening infective endocarditis. To treat oral biofilms, antibacterial mouth rinses are commonly used. Such initial biomaterial-bacteria interactions and the influence of antibacterial treatments are poorly understood and investigated here in situ by quartz crystal microbalance with dissipation monitoring (QCM-D). A saliva-coated titanium (Ti) biosensor is applied to analyze possible specific signal patterns indicating microbial binding mechanisms and bactericide-caused changes in bacterial film rigidity or cell leakage caused by a clinically relevant antibacterial agent (ABA), i.e., a mouth rinse comprising chlorhexidine (CHX) and cetylpyridinium chloride (CPC). Apparent missing mass effects during the formation of microscopically proven dense and vital bacterial films indicate punctual, specific binding of *S. gordonii* to the saliva-coated biosensor, compared to unspecific adhesion to pure Ti. Coincidentally to ABA-induced killing of surface-adhered bacteria, an increase of adsorbed dissipative mass can be sensed, contrary to the prior mass-loss. This suggests the acoustic sensing of the leakage of cellular content caused by bacterial cell wall rupturing and membrane damage upon the bactericidal attack. The results have significant implications for testing bacterial adhesion mechanisms and cellular integrity during interaction with antibacterial agents.

1. Introduction

Caused by bacteria adhering to implanted medical devices or to damaged tissue, invasive microbial infections, e.g., skin, lung or blood infections, are a major concern: the reasons are multifaceted, facing (i) the resistance of certain bacteria against so far effective antibiotics, (ii) current problems to develop in time adequate novel antibiotics, and (iii) insufficient approaches so far to attack bacteria once they are organized in biomedical biofilms (Fedtke et al., 2004; Stewart and Costerton, 2001; Tacconelli et al., 2018). In dentistry, disease-associated oral biofilms are a major concern (Jakubovics and Kolenbrander, 2010).

Dental tooth-root implants are widely used to support prosthetic superstructures such as crowns, bridges, or prostheses. However, implant-related infections such as peri-implantitis, which is an inflammatory condition of hard and soft tissue surrounding dental implants leading to a loss of supporting bone in a progressed stage, may compromise the long-term functionality and even cause implant failure (Zitzmann and Berglundh, 2008). The main reason for peri-implantitis is the presence of plaque (Sbordone and Bortolaia, 2003). Intrinsically harmless oral bacteria, such as the early colonizer *Streptococcus gordonii* (*S. gordonii)* which contributes to the base of oral biofilms (plaque) on implant and prosthetic surfaces (Foster and Kolenbrander, 2004), can also infiltrate towards subgingival sites into the bloodstream. There, they can trigger the formation of thrombus by platelet activation and aggregation, which might cause life-threatening infective endocarditis (Kerrigan and Cox, 2010). The reported epidemiology of peri-implantitis varies greatly within the literature, with numbers of affected implants ranging between 12% and 43% (Zitzmann and Berglundh,

* Corresponding author.
E-mail address: frank.rupp@med.uni-tuebingen.de (F. Rupp).

https://doi.org/10.1016/j.bios.2019.01.035
Received 23 November 2018; Received in revised form 7 January 2019; Accepted 13 January 2019
Available online 22 January 2019
0956-5663/

2008).

Due to the etiological relevance of bacterial adhesion and biofilm formation, therapies include the complete removal of infected tissue and bacterial films. Usually, a combination of conservative and surgical treatments is suggested encompassing different mechanical debridement and chemical decontamination methods (Heitz-Mayfield and Mombelli, 2014; Subramani and Wismeijer, 2012). For dental implant surgery, preoperative and postoperative mouth rinsing with chlorhexidine (CHX) has been regularly applied for the prophylaxis of peri-implantits. CHX is a cationic bisbiguanide with a wide spectrum of activity against gram-positive and gram-negative bacteria, yeasts, dermatophytes and some lipophilic viruses (Emilson, 1977). It is widely used in medicine for hand disinfection, preoperative skin cleansing preparation and mouth rinsing (Barbour et al., 2013). In dentistry, CHX has been used for plaque control, reducing caries and for gingivitis management with different formulations such as mouthwash, gel, and spray at different concentrations (0.1%, 0.12%, 0.2%) (Jones, 1997). At high concentrations, CHX is bactericidal due to its damaging effects to the cell membranes (Gjermo, 1989).

Studies indicate that titanium (Ti) might be involved in both uptake and release of CHX (Barbour et al., 2009) suggesting a certain antiplaque activity of titanium dental implants through prolonged CHX release. Cetylpyridinium chloride (CPC) is a cationic quarternary ammonium compound with antibacterial activity, also commonly used in mouth rinse to reduce bacterial plaque and gingival inflammation (Haps et al., 2008).

An important issue for early biofilm formation is that bacteria in most cases do not face the naked biomaterial surfaces but colonize surfaces that have been already conditioned by proteinaceous films or deposited exopolysaccharides.

In the oral cavity, all surfaces in contact with saliva are conditioned by a macromolecular thin film, the so-called pellicle (Lendenmann et al., 2000). However, during primary oral bacterial colonization, interactions between bacteria, salivary pellicle films, and antibacterial agents on Ti implant surfaces are still unclear in detail.

Label-free acoustic as well as optical transducers are commonly used to study biological responses at biomaterial/biosystem interfaces. The rationale for their selection depends on the aim of the respective study. Whereas acoustic methods such as quartz crystal microbalances (QCM) detect for example adsorbed wet mass, i.e, including the mass of solvent, surface plasmon resonance (SPR) considers the adsorbed dry mass. Furthermore, QCM with dissipation monitoring (QCM-D) allows insight into the stiffness of adsorbed films, which is of high interest when studying elastic/viscoelastic contacts or structures as developed during binding processes. QCM is a well-known nanogram sensitive technique that utilizes acoustic waves generated by oscillating a piezoelectric, single crystal quartz plate to measure, primarily, adsorbed mass (Dixon, 2008). This technique has been used in liquid systems for different applications in pharmaceutical, biological and biomedical fields (Becker and Cooper, 2011; Hussain et al., 2015, 2018)

Since a main focus of the present study was to investigate the stiffness of binding contacts of *S. gordonii* to pure titanium vs. saliva-coated titanium, where adsorbed water contributes to the detected signal development at the contact zone, QCM-D was chosen here.

In previous studies, we used QCM-D to investigate bacterial adhesion onto gold coated sensors (Krajewski et al., 2014). In that work, we observed mass-loss effects under certain binding conditions. These observations, contradictory on a first glance, make QCM-D a promising tool to differentiate specific punctual contacts of bacteria to a biosensor from unspecific binding effects. Sensors coated by different biomaterials can be used to investigate and compare binding interactions of bacteria with the respective conditioned biomaterials. Based on this, we hypothesize, that used as a biosensor featuring specific native receptors, QCM-D might be a suitable online instrumentation to shed light on how antibacterial agents modify regular bacterial adhesin-receptor binding. Another unsolved question is the potential of acoustic sensing to probe bacterial cell lysis by detection of leakage of cellular content as a consequence of cell wall and membrane damage, as recently shown for eukaryotic cells (Fatisson et al., 2011). Therefore, the present study sought for characteristic signal patterns that coincide with bacterial disintegration.

For proper simulations of the conditions in the oral cavity, it is of utmost importance to consider the above mentioned salivary pellicle as a functional, intermediate thin film. Hence, we decided to coat this salivary film directly online onto the QCM-D titanium sensors. The aim here was to generate a biosensor that enables native adhesin-receptor functionality at the outermost pellicle surface during subsequent bacterial adhesion and interaction with a clinically applied mouth rinse comprising CHX and CPC. This applied mouth rinse in the following is termed antibacterial agent (ABA). The common oral early colonizer *S. gordonii* (Foster and Kolenbrander, 2004) was chosen as model bacterium here. In addition to the QCM-D online experiments and the evaluation of pellicle-functionalized biosensors, after the respective QCM-D runs, the vitality of the adhered *S. gordonii* was analyzed by microscopy.

2. Material and methods

2.1. Online sensor system – quartz crystal microbalance

In this study, a commercial QCM-D device (qCell T; 3T analytik, Tuttlingen, Germany) was used for real-time monitoring of dynamic macromolecule-surface, bacteria-surface and macromolecule-bacteria interactions. Ti-coated quartz crystals with a resonance frequency f_0 of 10 MHz (3T analytik, Tuttlingen, Germany) were produced by sputter-coating. The sensors went through a sequence of ultrasonic water baths with 70% ethanol, 2% Hellmanex III (Hellma, Müllheim, Germany), and Millipore water, respectively, each for 5 min, and were finally dried under nitrogen prior to QCM-D experimental runs. Theoretically, the rigidly absorbed and evenly distributed masses causing frequency drops Δf below 0.2% of the resonant frequency f can be calculated by use of the Sauerbrey equation. The Sauerbrey factor of the applied quartz crystals is $C = 4.42\,ng\,cm^{-2}\,Hz^{-1}$. The theoretical sensitivity of the applied qCell T system is $0.87\,ng\,Hz^{-1}$. The quartz crystal is mounted into a thin, flexible polymer sheet for better handling and avoiding surface contamination or damage during experimental operations. The diameter of the sensor working area exposed to liquid is 8 mm.

A digital peristaltic pump (Reglo Digital MS-4/12, Ismatec, Wertheim, Germany) with adjustable flow was used for infusing different liquids under a temperature setting of 23 °C. The flow cell has an inner volume of 30 µl and is equipped with a window right above the sensor, allowing optical control of liquid filling of the cell.

2.2. Surface characterization of the sensors

The wettability of the applied Ti sputtered quartz crystal surfaces was analyzed by contact angle measurements, topography and roughness were analyzed by atomic force microscopy (AFM) and white light interferometry (WLI). Details can be found in the Supplementary material.

2.3. Bacterial suspension and antibacterial agent (ABA)

S. gordonii strain DL1 was grown at 37 °C as a stationary suspension culture in Schaedler medium (Becton Dickinson GmbH, Heidelberg, Germany). For the QCM-D experiments, bacterial cells were harvested by centrifugation for 5 min at 1560 g and resuspended in PBS (1×10^8 CFU ml^{-1}). The commercial mouth rinse GUM Paroex (Sunstar Deutschland GmbH, Schönau, Germany) comprising 0.12% chlorhexidine digluconate (CHX) and 0.05% cetylpyridinium chloride (CPC) was applied as ABA.

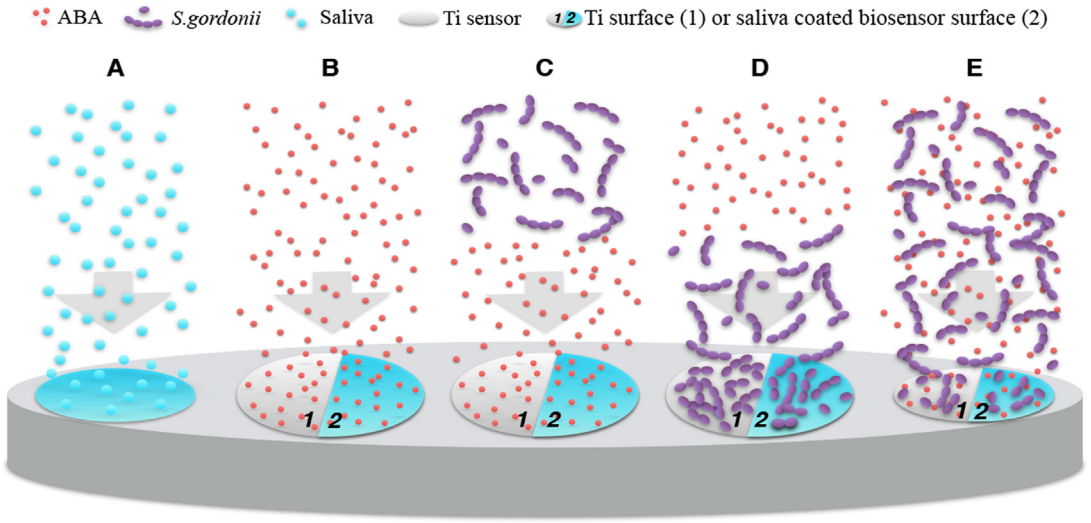

A: Online formation of saliva-coated Ti-based biosensors
B: ABA interacting with Ti sensors or with saliva-coated biosensors
B1: (ABA) PBS→ABA→PBS
B2: (Sal-ABA) PBS→Sal→PBS→ABA→PBS
C: *S. gordonii* interacting with Ti sensors or with saliva-coated biosensors, both pre-conditioned with ABA
C1: (ABA-S.g.) PBS→ABA→PBS→*S.g.*→PBS
C2: (Sal-ABA-S.g.) PBS→Sal→PBS→ABA→PBS→*S.g.*→PBS
D: ABA interacting with *S. gordonii* attached to Ti sensors or to saliva-coated biosensors
D1: (S.g.-ABA) PBS→*S.g.*→PBS→ABA→PBS
D2: (Sal-S.g.-ABA) PBS→Sal→PBS→*S.g.*→PBS→ABA→PBS
E: Mixture of ABA and *S. gordonii* interacting with Ti sensors or with saliva-coated biosensors
E1: (mixed ABA+S.g.) PBS→mixed ABA+*S.g.*→PBS
E2: (Sal-mixed ABA+S.g.) PBS→Sal→PBS→mixed ABA+*S.g.*→PBS
ABA (antibacterial agent), S.g. (*S. gordonii*), Sal (saliva), Ti (titanium).

Fig. 1. Schematic and respective protocols A-E showing the different experimental sequences of analytes perfused over titanium quartz crystal sensors in QCM-D runs. ABA (antibacterial agent), *S.g.* (*S. gordonii*), Sal (saliva), Ti (titanium).

2.4. QCM-D runs

The Ti-coated quartz crystals were placed into a window flow cell (qCell T, 3 T analytik, Tuttlingen, Germany) to form the bottom of the flow chamber. To start an experimental run, stable signal baselines during buffer rinsing with phosphate buffered solution (PBS) at a basic flow rate of 60 µl min^{-1} with a drift for the frequency below ± 2 Hz/min and for the dissipation below ± 5 Hz/min were defined as a prerequisite. Different protocols were applied with a different sequence of the analyte solutions that are perfused over the sensor, respectively (Fig. 1). The flowing time for human sterile saliva, PBS, and the antibacterial mouth rinse was 30 min, respectively, and for *S. gordonii* suspension it was 120 min. For experiments where *S. gordonii* and the applied ABA are initially mixed before the start of flow, 20 ml of harvested *S. gordonii* suspension were mixed with 5 ml of ABA. During the bacterial flowing time, the bacterial suspension in the storage vessel was constantly stirred. Between each run of analyte solutions, a rinsing step with PBS was conducted to remove loosely adsorbed molecular or loosely attached microbial mass.

2.5. Online assembling of the biosensor by coating with human saliva

In order to prevent time-related and interpersonal differences, human saliva was collected once from one healthy volunteer for the complete study, as previously described (Krajewski et al., 2014). Informed consent was obtained from the saliva donor. In short, collected saliva was filtered through a cell strainer (BD Falcon, BD Biosciences, Durham, NC, USA). The filtrates were centrifuged (4 °C, 14,000 g, 30 min). Then saliva was sterile-filtered by subsequent use of low protein binding syringe filters (Acrodisc Syringe Filters with Supor PES membrane; Pall, St Columb, UK) with decreasing pore diameters (5 µm, 1.2 µm, 0.45 µm). Finally, the obtained saliva was diluted 1:5 with phosphate-buffered saline (PBS; DPBS, Gibco®, Life Technologies, Darmstadt, Germany) and stored at − 18 °C. Saliva samples are homogenized through thawing and sonicating prior to the experiments. The Ti/saliva biosensors were built online under QCM-D controlled flow for 30 min by adsorption of salivary macromolecules and the formation of the so-called pellicle film.

2.6. Live/Dead staining and microscopic analysis

After termination of the respective QCM-D experiments with bacteria, the quartz sensors were demounted from the flow cell and stained by Live/Dead BacLightTM Viability kit (Molecular Probes®, Life Technologies). After staining, samples were examined with a fluorescence microscope (Optiphot-2, Nikon, Tokyo, Japan) equipped with a remote control DSLR (Nikon 550D). To visualize the stained microorganisms, a filter combination with 450–490 nm excitation band-pass filter and a 520 nm high-pass emission filter (Nikon B2 Filtercube) was used.

2.7. Scanning electron microscopy (SEM) and field-emission SEM microscopy (FE-SEM)

After QCM-runs, the sensors were demounted from the flow-cell. The samples were then fixed in glutaraldehyde solution (2% in PBS, pH 7.4) at 4 °C for 20 h. After washing with PBS, the samples were dehydrated in ascending series (30%, 40% 50% 60% 70%, 80%, 90%, 96%, 100%) of ethanol, then critical-point-dried in an E 3100 Critical Point Dryer (Quorum Technologies, Laughton, UK), and subsequently sputter-coated (SCD 050, Baltec, Germany) with a thin Au–Pd layer. The specimens were analyzed in a scanning electron microscope (Leo 1430 SEM, Zeiss, Oberkochen, Germany) and an FE-SEM (JSM-6500F, Jeol, Japan).

2.8. Dissipation-frequency (ΔD-Δf) plots

After the measurement, ΔD (y-axis)-Δf (x-axis) plots are drawn. The quotient of ΔD and Δf ($\Delta D/\Delta f$) represents the viscosity or rigidity of the adsorbed films or molecules (Marcus et al., 2012). Forming completely rigid homogeneous layers contributes to a change in frequency combined with an unchanged, constant dissipation. An increase of the softness and water content of surface bound films, on the other hand, leads to a decrease of frequency and increase of dissipation. If the ΔD-Δf plot points to a dissipation decreasing direction, the film tends to become more rigid, and vice versa. Concurrently, if the ΔD-Δf plot points to a frequency decreasing direction, this represents mass loading on the film, and vice versa (McCubbin et al., 2011).

2.9. Statistical analysis

All QCM-D experiments were repeated for at least 5 times with the exception of the experiments where ABA was mixed with *S. gordonii* suspension. These QCM-D runs were repeated three times. Data were basically described by means and respective standard deviations. Differences between means of frequency and dissipation in different groups were statistically analyzed with one-way analysis of variance (ANOVA) and post-hoc test (Tukey analysis). Differences were regarded as statistically significant when $p < 0.05$.

3. Results

Surface analytical results of the hydrophilicity and roughness of the titanium-coated QCM-D sensors are shown in the Supplementary materials (Fig. S1). Fig. 2 below summarizes the detected frequency and dissipation signal development during the different QCM-D runs. Detailed results of the frequency and dissipation shifts are summarized in Table S1 and Fig. S2 (Supplementary materials).

3.1. Saliva-surface and ABA-surface molecular interactions

After reaching the pre-defined baseline criteria with PBS, saliva flow was applied for a period of 30 min, followed by a final 30 min rinsing step with PBS. After onset of saliva flow, the frequency decreased and dissipation increased reaching equilibrium values. No significant desorption was observed in the course of PBS rinsing, indicating an irreversible salivary pellicle formation on the Ti surface. These saliva-coated sensors were used in the study as biosensors to detect specific, pellicle-mediated surface interactions of ABA and bacteria.

The interaction of the antibacterial mouth rinse with the Ti surface appears as a kind of “U”-shaped frequency signal with a characteristic fast frequency decrease and fast frequency increase upon PBS rinsing (first 60 min of reaction time in Fig. 2c) reaching nearly the original baseline level. In contrast, the dissipation signal increased and reached equilibrium, then, upon PBS it decreased sharply to the level of the baseline.

ABA interaction with a salivary conditioned biosensor surface is shown in the first 120 min reaction time in Fig. 2d. The ABA caused a sharp decrease of frequency and a sharp increase of dissipation, both reaching equilibrium. Upon PBS flow, a sudden increase of frequency and a sudden decrease of dissipation occurred.

3.2. Influence of salivary pellicle and ABA on S. gordonii adhesion and vitality

After 120 min flow, *S. gordonii* (*S.g.*) caused a frequency drop and an increase of dissipation resulting in steady state equilibrium (Fig. 2a). The frequency decrease represents mass loading by the attachment and further adhesion of *S. gordonii*. No obvious desorption process was found, the frequency and dissipation kept stable during the following PBS rinsing. Fluorescence microscopy after Live/Dead staining showed green and dense bacterial films on the Ti coated sensor surfaces (Fig. 3a).

Quite different results were obtained when *S. gordonii* adhered now on the salivary conditioned biosensor surface for 120 min (Fig. 2b). The dissipation slightly increased, however, the frequency increased now similarly, indicating here mass-loss instead of mass loading. Nevertheless, according to microscopic analysis, Live/Dead staining shows surface-adhered, green stained and thus alive bacteria, with slightly lower density than on unconditioned Ti (Fig. 3b). On a titanium surface pre-treated with antibacterial mouth rinse, *S. gordonii* induced a frequency decrease and a dissipation increase (Fig. 2c). The *S. gordonii* films formed here are dense and stained green, similar to the bacterial films observed on the pure Ti surface without ABA pre-treatment. Thus, almost all bacteria retained on the surface are alive (Fig. 3c).

In the next experimental run, the saliva-coated biosensor was pre-treated with ABA (see also protocol B2). At this surface, *S. gordonii* caused a slight increase of both frequency and dissipation (Fig. 2d). *S. gordonii* appears in a dense layer on the surface, predominantly in green color (Fig. 3d).

After a typical signal development during 120 min film formation of *S. gordonii*, characterized by an increase of dissipation and a decrease of frequency, ABA caused a sharp decrease of frequency along with a sharp increase of dissipation (Fig. 2e). Upon PBS rinsing, a sharp increase of frequency and a sharp decrease of dissipation occurred. Fluorescence microscopy disclosed dense red stained biofilms of *S. gordonii* on the surface (Fig. 3e).

After *S. gordonii* was pre-adhered to the saliva-coated biosensor, ABA caused similar huge signal changes, also followed by fast reversibility upon the start of PBS flow (Fig. 2f). Microscopic results showed a dense and completely red stained film of *S. gordonii* (Fig. 3f). Thus, after rinsing with the bactericidal solution, all surface-adhered bacteria were killed. However, no obvious morphological changes of *S. gordonii* after ABA treatment were observed by SEM and FE-SEM (Fig. 4).

Fig. 2g shows QCM-D signals during 120 min interaction of a mixture of ABA and *S. gordonii* with the Ti sensor surface. After fast decrease of frequency, lasting for approximately 5 min, and a fast increase of dissipation upon PBS rinsing, the equilibrated signals showed partial reversibility, with a sharp increase of frequency, and a sharp decrease of dissipation. According to Live/Dead staining, *S. gordonii* is killed and attached to the surface in relatively low density (Fig. 3g).

When the bacteria/bactericide mixture reached the saliva-coated biosensor surface, both frequency and dissipation showed a positive signal drift during the 120 min flow. The following rinsing with PBS contributed to a small increase in frequency and a small drop in dissipation (Fig. 2h). The bacterial films were of a medium density and completely red stained (Fig. 3h).

3.3. Rigidity of formed films

The $\Delta D/\Delta f$ slopes of ABA, saliva, and *S. gordonii* interacting with pure Ti are all negative, characterized by decreasing frequencies and increasing dissipations during interaction (Fig. 5). A significant

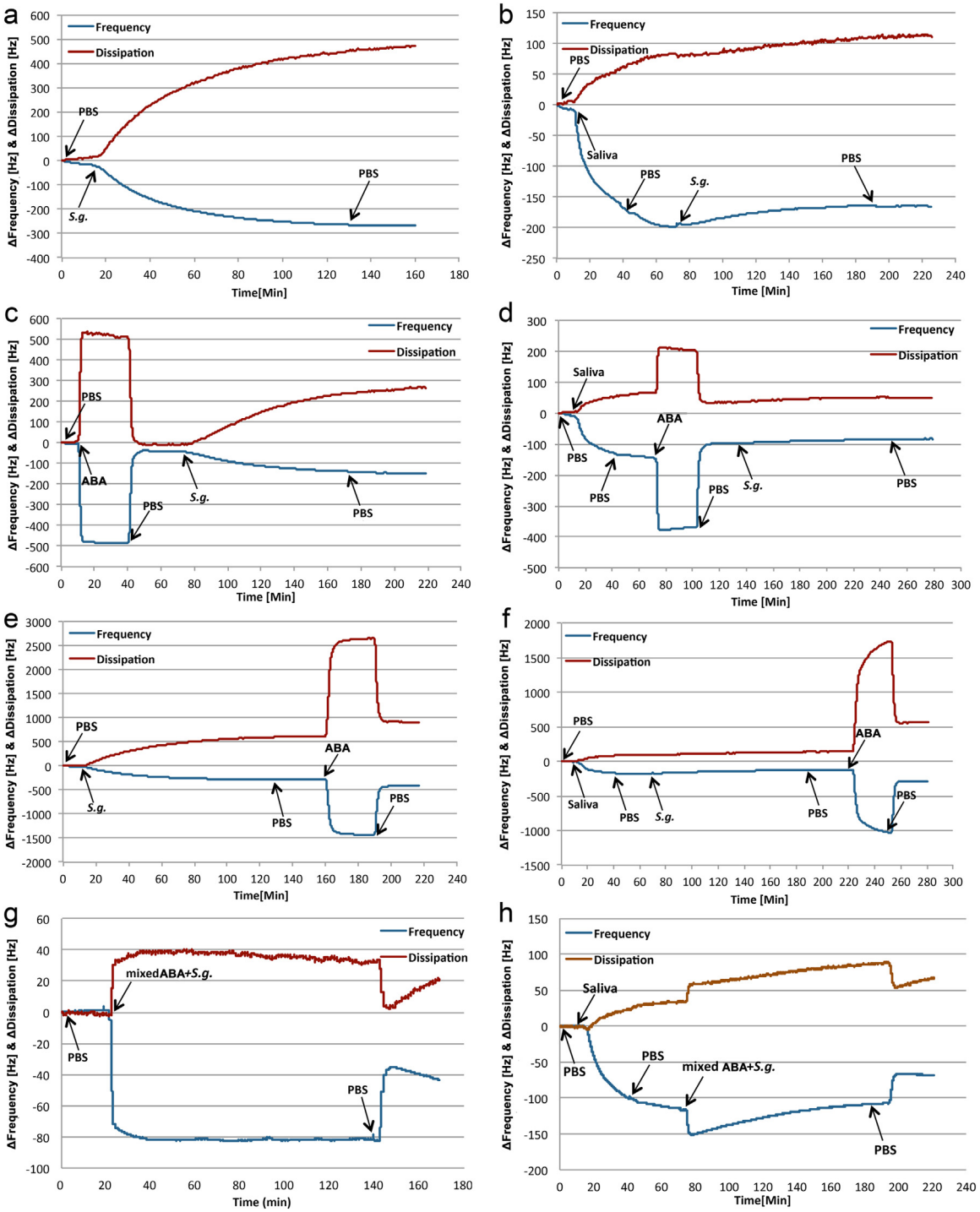

Fig. 2. Exemplary measurements with frequency and dissipation output of ABA, saliva and *S. gordonii* in different flow sequences on Ti. **a. *S.g.* (protocol D1):** *S. gordonii* interaction with Ti; **b. Sal-S.g (protocol D2):** *S. gordonii* interaction with the saliva-coated biosensor; **c. ABA-*S.g.* (protocol C1):** *S. gordonii* interaction with Ti that was pre-conditioned with bactericidal agent; **d. Sal-ABA-*S.g.* (protocol C2):** *S. gordonii* interacting with the biosensor that was pre-conditioned with bactericidal agent; **e. *S.g.*-ABA (protocol D1):** *S. gordonii* interaction with Ti followed by interaction with bactericidal agent; **f. Sal-*S.g.*-ABA (protocol D2):** *S. gordonii* interaction with the saliva-coated biosensor followed by interaction with bactericidal agent; **g. Mixed ABA + *S.g.* (protocol E1):** mixture of *S. gordonii* and bactericidal agent interacting with Ti; **h. Sal-mixed ABA + *S.g.* (protocol E2):** mixture of *S. gordonii* and bactericidal agent interacting with the saliva-coated biosensor. ABA (antibacterial agent), *S.g.* (*S. gordonii*), Sal (saliva), Ti (titanium).

exception from this signal pattern that reflects mass loading has been found in the interaction of *S. gordonii* with the saliva-coated biosensor, where the frequency slightly increased during adhesion indicating mass-loss (Fig. 5b, d).

Comparing the impact of antibacterial agent on the rigidity of bacterial films, the slopes indicate a slightly higher film rigidity on pure Ti (Fig. 5c) compared to a film formed on Ti that was pre-conditioned by ABA (Fig. 5a). The agent further increases the rigidity of bacterial films if applied onto an already formed film (Fig. 5c). In cases it acts on a film with bacteria bound to pure Ti as shown in Fig. 5c compared to bacteria specifically bound to a pre-adsorbed salivary film (Fig. 5d), the latter appears slightly more dissipative. Furthermore, the interaction of

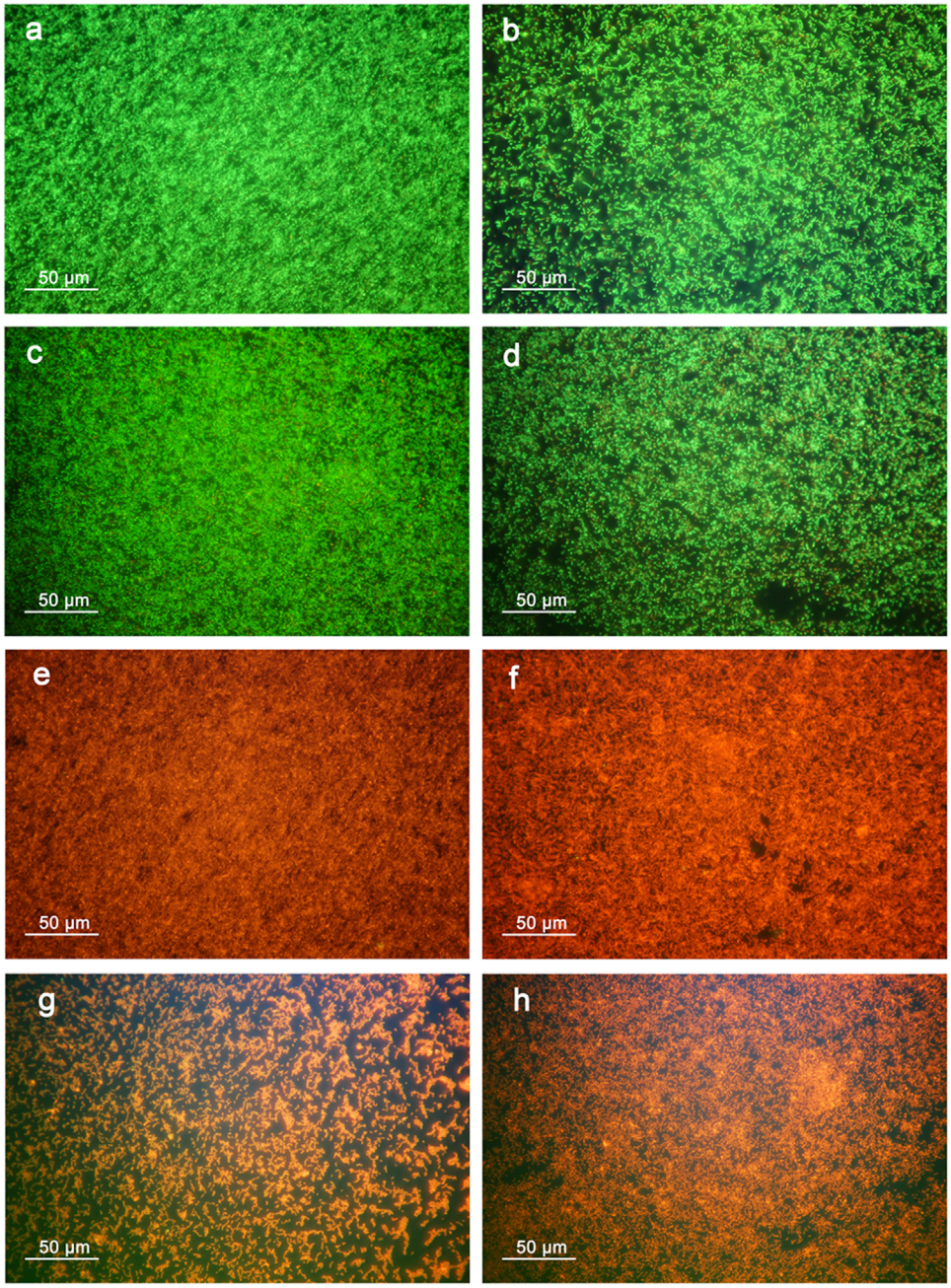

Fig. 3. Fluorescent microscopic images of Live/Dead stained bacteria. **a. *S.g.* (protocol D1):** *S. gordonii* interacting with Ti; **b. Sal-*S.g.* (protocol D2):** *S. gordonii* interacting with the saliva-coated biosensor; **c. ABA-*S.g.* (protocol C1):** *S. gordonii* interacting with Ti preconditioned with bactericidal agent; **d. Sal-ABA-*S.g.* (protocol C2):** *S. gordonii* interacting with the saliva-coated biosensor that was preconditioned with bactericidal agent; **e. *S.g.*-ABA (protocol D1):** ABA interacting with *S. gordonii* attached to Ti; **f. Sal-*S.g.*-ABA (protocol D2):** ABA interacting with Ti preconditioned with saliva followed by *S. gordonii* attachment; **g. Mixed ABA + *S.g.* (protocol E1):** mixture of *S. gordonii* and bactericidal agent interacting with Ti; **h. Sal-mixed ABA + *S.g.* (protocol E2):** mixture of *S. gordonii* and ABA interacting with the saliva-coated biosensor. ABA (antibacterial agent), *S.g.* (*S. gordonii*), Sal (saliva), Ti (titanium).

bactericide in both cases is not fully reversible as observed on pure Ti (Fig. 5a) and on the biosensor, where it increased the softness of the pellicle film to a low extent (Fig. 5b). This irreversibility observed in Fig. 5c and d indicates at the end of the interaction with *S. gordonii* that the antibacterial agent has caused a significant increase of adsorbed, dissipative mass.

4. Discussion

To our best knowledge, this is the first implant related study that investigates the impact of an antibacterial mouth rinse comprising CHX and CPC on the adhesion and cellular integrity of *S. gordonii* by an acoustic sensor system. The clinical relevance in this online study was enhanced by including salivary pellicle films. These macromolecular films are physiologically formed in saliva contact as intermediate layers between implant surfaces and colonizing bacteria and were applied here to probe specific interactions during bacterial adhesion to pellicle macromolecules. The applied concentration of the model bacterium *S. gordonii* of 1×10^8 CFU/ml corresponds to the total concentration of Streptococci in saliva. The overall concentration of bacteria in saliva is estimated to 1×10^9 bacteria/ml (Berg, 1996).

4.1. *S. gordonii* / pellicle interaction and mass-loss effects

The Ti coated sensors used here were moderately hydrophilic allowing simulation of intraoral pellicle formation in this in vitro model. The acquired pellicle is normally formed on any natural and artificial dental material surfaces exposed to the oral salivary environment and consists of spontaneously adsorbing, protein-dominated films. This pellicle plays an irreplaceable role in oral bacterial adhesion and dental plaque formation (Lendenmann et al., 2000; Rupp et al., 2012). In the present study, to simulate the formation of pellicle on a Ti implant surface under clinical conditions, human sterile saliva was adsorbed for entire 30 min on the Ti coated sensors.

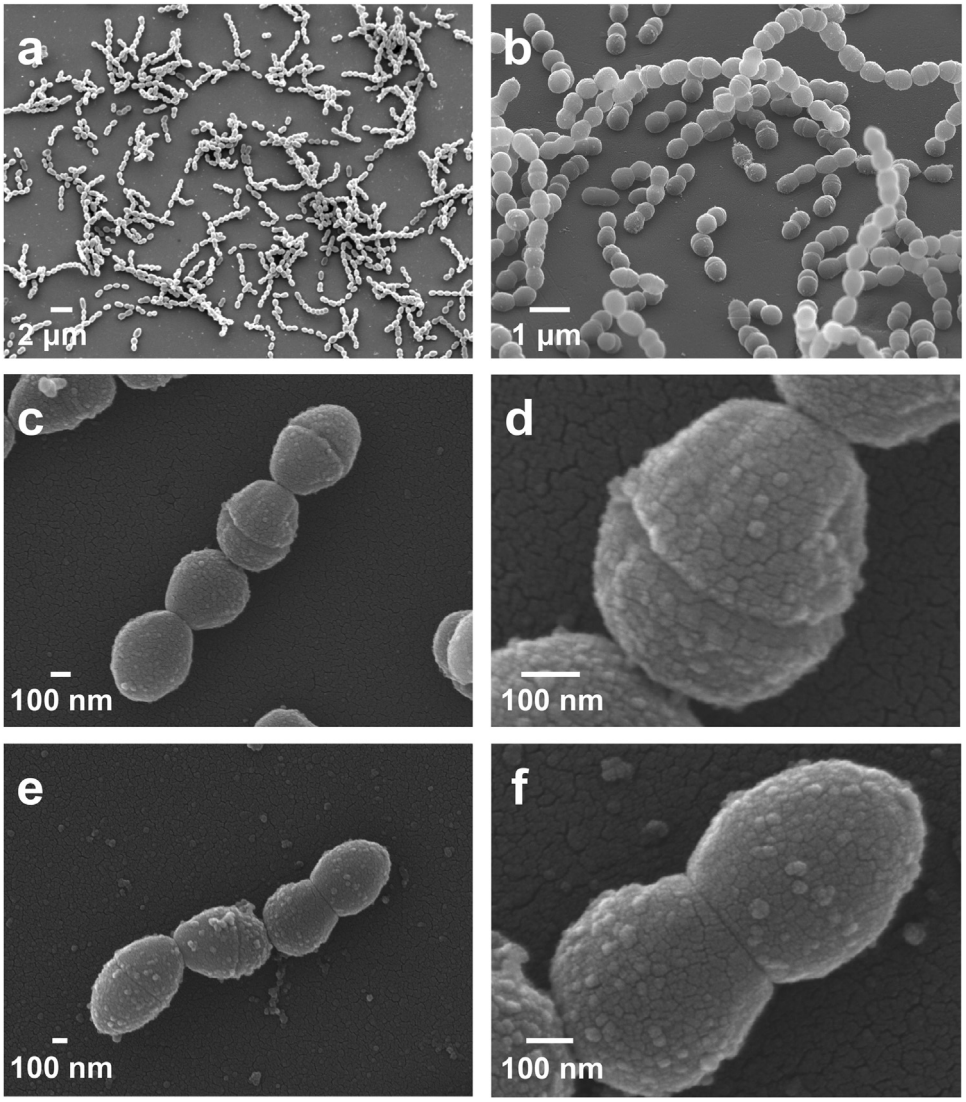

Fig. 4. SEM and FE-SEM images of *S. gordonii* on saliva conditioned biosensor surfaces before (e, f) and after treatment with ABA (a-d). Both groups went through subsequent fixation, critical point drying, and sputter-coating. a. 5000× SEM; b. 10,000× FE-SEM; c. 43,000× FE-SEM; d. 150,000× FE-SEM; e. 40,000× FE-SEM; f. 120,000× FE-SEM.

The QCM-D results showed that saliva adsorbed irreversibly onto Ti without obvious desorption upon PBS rinsing. The preconditioning with saliva resulted in 537 ng/cm^2 of retained mass, confirming earlier results (Rupp et al., 2012). As depicted in Fig. 6, saliva derived pellicle is a heterogeneous multilayered structure with an inner denser basal layer and a highly hydrated outermost layer (Cardenas et al., 2007) comprising larger proteins. In a previous study, we quantified the thickness of such pellicle films on Ti by Kelvin-Voigt modelling of QCM-D data to be < 30 nm (Rupp et al., 2012).

As shown in our results, *S. gordonii* adhered to a slightly lesser degree onto pellicle than on pure Ti. *S. gordonii* adhesion to a pellicle induced a simultaneous small increase of both frequency and dissipation, which formally represents mass-loss. Apparent mass-loss in the face of microscopically proven surface-adhered bacteria points to specific interactions between *S. gordonii* and the pellicle film. Similar frequency increases were reported recently for *S. gordonii* adhesion to gold pre-conditioned with saliva (Krajewski et al., 2014). Our results indicate that the applied biosensors constitute a sensing probe for specific adhesion of *S. gordonii* by exposing receptors at their outermost surface complementary to adhesins of *S. gordonii*. Whether this biosensor allows specific adhesion of other bacteria has to be proven in further studies.

Compared to two-layer viscoelastic models of cells, mass-loss during adhesion of rigid, particle-like bacteria might better be explained based on a coupled-oscillator model (Tymchenko et al., 2012): particle-resonator systems can mathematically be modeled as a pair of coupled oscillators, which show for weak particle binding an increase of system frequency (Dybwad, 1985). This soft contact is based, due to this model, on a resonance frequency of the particle below the resonance frequency of the QCM sensor due to a low stiffness (low spring constant) of the bacterium-sensor binding (Olsson et al., 2011). Positive frequency shifts of bacteria were observed on *Streptococcus salivarius mutants* with surface appendages of different length, with mass loading for bare bacteria and frequency increase up to positive shifts dependent on the type of appendages (Olsson et al., 2009). Such bacteria do not directly contact the sensor surface and are kept at a certain distance.

Approximately 35% of *S. gordonii* DL1 (wild type) cells are equipped with short peritrichous fibrils (fibrillae) having a length of an estimated 60–80 nm (McNab et al., 1999). In addition, the pre-adsorbed viscoelastic salivary film increased the distance between the bound bacteria and the oscillating sensor surface. Furthermore, gram positive *S. gordonii* has a 30–50 nm thick peptidoglycan cell wall structure (Vollmer et al., 2008). Thus, most bulk parts of the bacterium are outside the penetration depth of the applied 10 MHz QCM-D evanescence shear wave, which in an aqueous system amounts to about 180 nm.

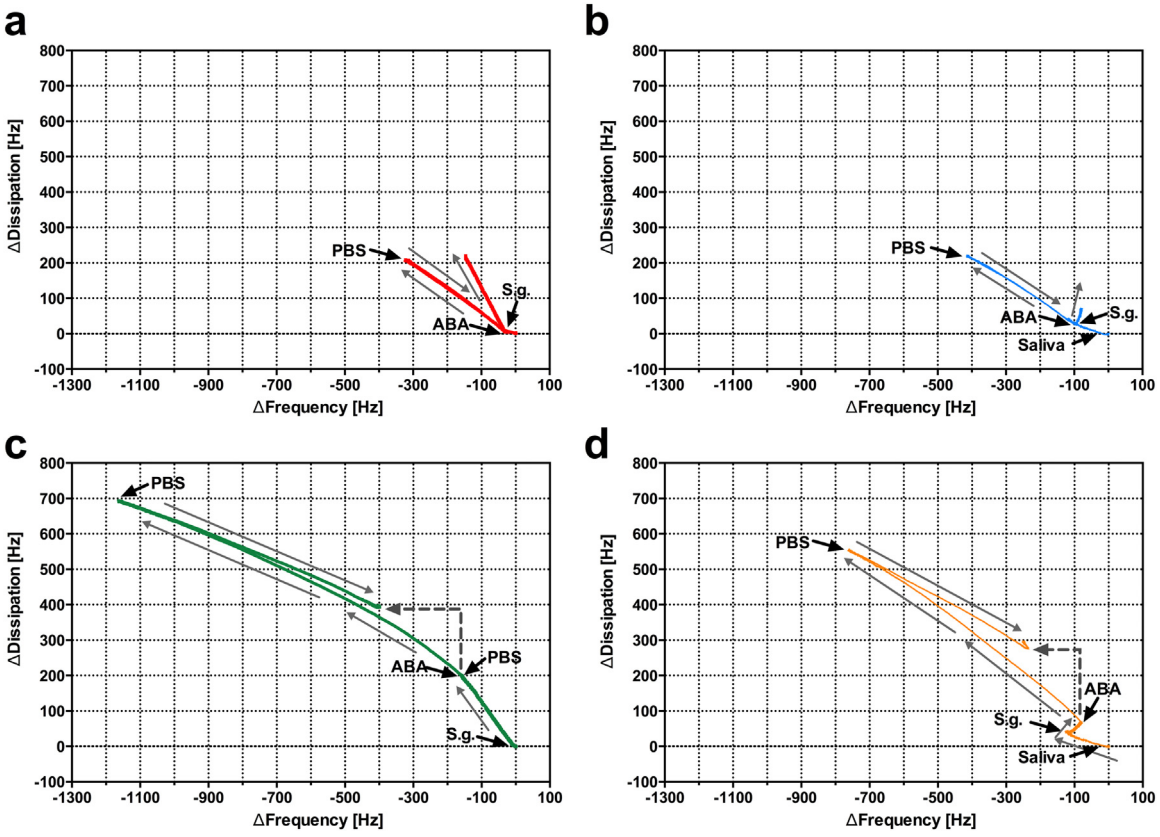

Fig. 5. Film stiffness during QCM-D mass-loading or mass-loss processes (ΔD-Δf plots) of exemplary measurements. The gray arrows indicate the progress of ΔD-Δf in the course of a measurement. The gray dashed lines represent the partial irreversibility of ABA and *S. gordonii* interaction, causing final mass loading. The black arrows show the infusion of different analyte solutions: **a.** ABA-*S.g.*, **b.** Sal-ABA-*S.g.*, **c.** *S.g.*-ABA, **d.** Sal-*S.g.*-ABA. ABA (antibacterial agent), *S.g.* (*S. gordonii*), Sal (saliva), Ti (titanium).

Therefore, mass loading and viscoelastic properties cannot be fully detected by the acoustic QCM-D sensor (Krajewski et al., 2014) (Fig. 6).

According to the coupled resonator model, positive frequency shifts require small-point contacts between micrometer-sized adsorbed particles and the sensor surface (Pomorska et al., 2010). *S. gordonii* binds to constituents of the pellicle by proteinaceous adhesins, whereby their specific stereochemical binding mechanism contributed to small contact areas (Ahn et al., 2003; Ruhl et al., 2004; Herzberg, 2000): In *S. gordonii*, variants of serine-rich (Srr) protein adhesins or adhesins belonging to the antigen I/II family bind to salivary receptors (Nobbs et al., 2011). It is still unclear why different bacteria show partially adhesion to pure substrates such as gold or titanium by conventional mass loading with frequency related to the adsorbed mass, e.g., *S. gordonii* on gold (Krajewski et al., 2014) and Ti (current study), *S. salivarius* without surface appendages on gold (Olsson et al., 2009), and partially according to the coupled oscillator model, where the frequency represents the contact stiffness and mass-loss effects can be observed, e.g., *S. salivarius* with surface appendages on gold (Olsson et al., 2009), *S. gordonii* on pellicle (current study), and *P. aeruginosa* on hydrophilic silica or more hydrophobic polyvinylidene fluoride (Marcus et al., 2012).

The increase of dissipation during bacterial interaction is large on pure Ti but very low with pellicle as an intermediate film. Bacterial films formed by unspecific binding seem to be more dissipative, whereas specific binding increases film stiffness. This might once more be due to the limited detection of the bacteria by the shear wave. Furthermore, coupled oscillators reflect now the interfacial binding between bacteria and the sensor rather than the attached particle mass or dissipation.

As highlighted in Fig. 6, bacteria binding primarily to the surface of a heterogeneous pellicle film lead to a perpendicularly heterogeneous layer with increasing complexity by additional colonizing bacterial species. Furthermore, there is also inhomogeneity horizontally to the sensor surface due to at least initially inhomogeneously distributed bacteria in the lateral direction. Currently, there are no models available which are able to quantitatively describe the respective QCM data upon such complex layer formation (Reviakine et al., 2011).

4.2. Surface interaction of antibacterial agent and its impact on bacterial adhesion and vitality

CHX can interact with tooth, pellicle, bacteria (Kozlovsky et al., 2006) and Ti. Compared with positively charged CHX, in a healthy oral environment with pH 6.7–7.3 (Baliga et al., 2013) the Ti surface is normally slightly negatively charged (Cecilia Yan Guo and Hong Tang, 2012; Preočanin and Kallay, 2006). This supports binding of CHX and of other cationic bactericidal agents such as CPC to the Ti surface. CHX in PBS can rapidly adsorb to crystalline TiO_2 reaching equilibrium within 60 s followed by a gradual desorption process (Barbour et al., 2007).

According to our QCM-D results, ABA causes a typical fast frequency decrease and dissipation increase for different surface conditions, i.e., pure Ti, pellicle-coated Ti, or adhered *S. gordonii* films. The fast frequency decrease induced by ABA on pure Ti mainly originates from differences in the viscosity between the bactericidal solution and PBS, indicated by fast and symmetrical frequency and dissipation shifts, and only to a limited degree due to molecular adsorption. The observed QCM signal developement, including its reversibility on pellicle, is in line with a previous study using ellipsometry (Freitas et al., 1993).

Studies indicate that CHX binds to a higher degree on rough

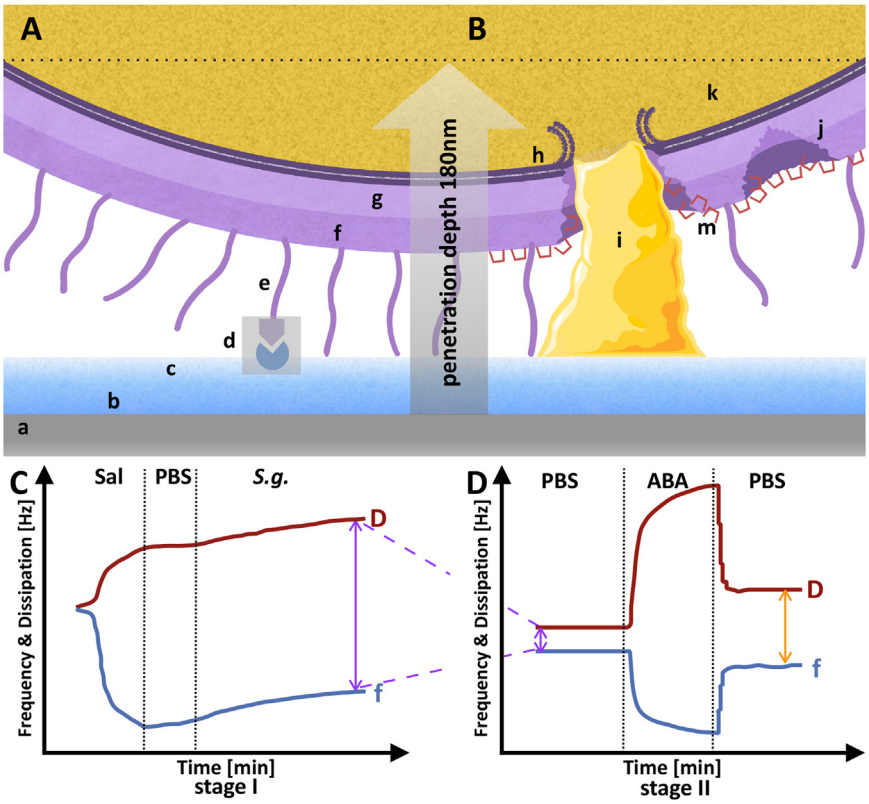

Fig. 6. Schematic illustration of QCM-D signal patterns during two physiologically important oral situations: First, specific interaction of *S. gordonii* and pellicle (A) and the respective QCM-D signals (C) are shown. Second, the impact of the bactericidal agent ABA on *S. gordonii* pre-adhered to pellicle (B) with the observed characteristic QCM-D response (D) are presented. Please note that C and D highlight two consecutive parts (**stage I** and **stage II**) of one connected online measurement as shown in Fig. 2f; therefore, the purple arrows in C and D represent the same gap between D and f. The gap is widened by the interaction of ABA with *S. gordonii*. Details: the transparent gray central arrow subdividing A and B illustrates the penetration depth of the evanescent acoustic shear wave into the biological interface, which is about 180 nm (Krajewski et al., 2014). **a.** Ti coated sensor surface; **b and c**. salivary pellicle coating with a dense basal layer (b) and a highly hydrated outermost layer (c) with entire pellicle thickness of < 30 nm (Rupp et al., 2012); **d.** exemplary specific interaction of bacterial adhesin and pellicle receptor; **e.** peritrichous fibrils of *S. gordonii* 60–80 nm in length (Krajewski et al., 2014; McNab et al., 1999); **f.** peptidoglycan (outer wall zone) 15–30 nm thick; **g.** peptidoglycan (inner wall zone, periplasmic space) 16–22 nm thick (Vollmer et al., 2008); **h**. bacterial plasma phospholipid bilayer membrane, about 4 nm thick; **i.** disintegration of both peptidoglycan cell wall and plasma membrane causing leakage of bacterial plasmatic components; **j.** perforation of bacterial peptidoglycan; **k.** bacterial plasma (not shown are intracellular components like DNA and ribosomes); **m.** U-shaped, red colored ABA molecules interacting with the outer cell wall. **Stage I** in **C** represents the specific binding of *S. gordonii* onto the saliva coated biosensor (modeled in A) characterized by mass-loss (coincident increase of frequency and dissipation) and explained by the coupled-oscillator model. **Stage II** in **D** represents the impact of ABA on pellicle-bound *S. gordonii*, with the characteristic final frequency decrease and dissipation increase which indicates contrary to stage I mass loading. As outlined in the text, mass loading may reflect coincident cell damage and cytoplasm release (modeled in B). ABA (antibacterial agent), *S.g.* (*S. gordonii*), Sal (saliva), Ti (titanium).

compared to smooth surfaces, due to an increased surface area and a higher number of possible binding sites (Barbour et al., 2009, 2007; Freitas et al., 1993; Kozlovsky et al., 2006). Smooth Ti as used in our study to simulate the transgingival part of dental implants, seems to offer only a limited number of binding sites for ABA. However, for clinical use, very smooth trans-gingival implant surfaces have been suggested to inhibit the accumulation and maturation of plaque (Rimondini et al., 1997). To find a balance between functionally sufficient retention of bactericides and lesser roughness-induced plaque accumulation, the modification of smooth Ti with topographical features on the nanoscale appears to be a promising, sophisticated approach that should be investigated further.

Joiner et al. reported that CHX adsorbs to the pellicle and contributes to modified pellicle properties, such as increased electrostatic attractions and interactions between cationic CHX and negatively charged components (Joiner et al., 2006). After rinsing with CHX, saliva itself exerts antibacterial activity for up to 5 h, the persistence in oral surfaces could suppress salivary bacterial counts for over 12 h (Roberts and Addy, 1981) showing the reversibility of CHX binding towards saliva (Joiner et al., 2006).

CHX inhibits bacterial aggregation and attachment through binding to oral surfaces and precipitating agglutination molecules in saliva by the displacement of Ca^{2+} (Decker et al., 2003; Rolla and Melsen, 1975; Winrow, 1973), which explains the lower bacterial density and diminished frequency changes in our study observed upon ABA/bacteria mixtures.

The mechanisms of CHX and CPC for killing bacteria include adsorption to the negatively charged bacterial cell wall, damaging the permeability barriers which form the entrance of bactericides to the cytoplasm, precipitation and leakage of the cytoplasm, and inhibition of cell wall and membrane rehabilitation (Cheung et al., 2012; Davies, 1973; Denyer, 1995; Pitten FA, 2001).

Bactericidal effects have been confirmed in our study by the observed efficient killing of planktonic as well as surface-adhered *S. gordonii* by bactericidal agent. For interaction of the ABA with the pre-adsorbed bacteria, QCM-D disclosed partial irreversibility of both frequency and dissipation. By a final decrease in frequency and an increase in dissipation, this indicated mass loading, independent if bacteria adhered unspecifically on pure Ti or specifically on salivary films. Simultaneously, the bacteria-pellicle multilayer becomes slightly stiffer by the bactericidal solution as shown by the decreased slope of the ΔD-Δf plots. These QCM-D results may be indications of the outlined irreversible microbial cell wall damage and cytoplasm release, common mechanisms of biocide interaction. Thus, the observed increase of detectable mass upon ABA may likely be due to leakage of cell content through breached, damaged sites of the cell wall and the ruptured membrane (Fig. 6). Similar to our findings, Olsson et al. have shown that *Staphyloccocus epidermis* adheres to gold sensor surfaces according to the coupled oscillator theory and shows conventional mass-loading in course of leakage of extracellular polymeric substances (Olsson et al., 2011). Ultrastructural studies by transmission electron microscopy (TEM) have shown that CHX caused membrane rupturing and blebbing to a minor part of bacteria within oral biofilms, while CHX did not contribute to a significant disintegration of mature oral biofilms (Vitkov et al., 2005). In contrast to TEM, and in agreement with our FE-SEM results, no CHX caused cellular damage could be observed in the study of Vitkov et al.

5. Conclusions

The QCM-D online system with saliva-coated biosensors provides a useful assay to investigate in vitro dynamic interfacial processes located in the oral environment, such as salivary pellicle formation, bacterial adhesion, and effects of antibacterial agents.

This assay provides mechanistic insight not only for conventional mass loading processes; additionally, important information about binding mechanisms of bacteria is provided in the case of dissipative events. Due to missing-mass effects and strong influence of a complex viscoelastic multilayer system, bacteria that colonize implant surfaces cannot be simply counted by QCM-D. Important complementary information about microbial film formation can be received by microscopy. Missing-mass effects as observed during bacteria/pellicle interaction indicate specific adhesion mechanisms between bacterial adhesins and complementary salivary receptors.

During killing of the model bacterium *S. gordonii* by the applied antibacterial agent, QCM-D could sense mass adsorption, most likely due to concurrent release of cell content towards the sensor caused by cell wall and membrane rupture. Therefore, QCM-D is bearing potential for further mass and dissipation sensitive studies concerning the impact of antibacterial agents on the integrity of gram-positive and gram-negative bacteria.

To provide controlled parameters for high reproducibility, suspensions of a single bacterium in standardized buffer solutions were investigated in a basic model system. In future experiments, the adhesion of different bacteria suspended additionally in processed or natural human saliva instead of simple buffer solutions have to be investigated to highlight adhesion directly from this bioliquid and to expand this assay.

Acknowledgements

This work was supported by AiF ZIM, Germany (KF2806411CR4). X.Z. is supported by the China Scholarship Council (201708080003). We acknowledge Ingrid Stephan and Ernst Schweizer for technical assistance in our laboratories.

Conflict of interest

The author Frank K. Gehring is shareholder of 3T analytik (Germany) and participated in this study as an active scientific collaborator. The authors do not have any financial or personal conflict of interest.

Appendix A. Supporting information

Supplementary data associated with this article can be found in the online version at doi:10.1016/j.bios.2019.01.035.

References

Ahn, S.J., Kho, H.S., Kim, K.K., Nahm, D.S., 2003. Am. J. Orthod. Dentofac. Orthop. 124, 198–205.
Baliga, S., Muglikar, S., Kale, R., 2013. J. Indian Soc. Periodontol. 17, 461–465.
Barbour, M.E., O'Sullivan, D.J., Jagger, D.C., 2007. Colloids Surf. A 307, 116–120.
Barbour, M.E., Maddocks, S.E., Wood, N.J., Collins, A.M., 2013. Int. J. Nanomed. 8, 3507–3519.
Barbour, M.E., Gandhi, N., el-Turki, A., O'Sullivan, D.J., Jagger, D.C., 2009. J. Biomed. Mater. Res. A 90, 993–998.
Becker, B., Cooper, M.A., 2011. J. Mol. Recognit. 24, 754–787.
Berg, R.D., 1996. Trends Microbiol. 4, 430–435.
Cardenas, M., Arnebrant, T., Rennie, A., Fragneto, G., Thomas, R.K., Lindh, L., 2007. Biomacromolecules 8, 65–69.
Cecilia Yan Guo, J.P.M., Hong Tang, Alexander Tin, 2012. Int. J. Biomater. 2012, 5.
Cheung, H.-Y., Wong, M.M.-K., Cheung, S.-H., Liang, L.Y., Lam, Y.-W., Chiu, S.-K., 2012. PLoS One 7 (e36659).
Davies, A., 1973. J. Periodontics Res. Suppl. 12, 68–75.
Decker, E.-M., Weiger, R., Von Ohle, C., Wiech, I., Brecx, M., 2003. Clin. Oral. Investig. 7, 98–102.
Denyer, S.P., 1995. Int. Biodeterior. Biodegrad. 36, 227–245.
Dixon, M.C., 2008. J. Biomol. Tech. 19, 151–158.
Dybwad, G.L., 1985. J. Appl. Phys. 58, 2789–2790.
Emilson, C.G., 1977. Eur. J. Oral Sci. 85 (4), 255–265.
Fatisson, J., Azari, F., Tufenkji, N., 2011. Biosens. Bioelectron. 26, 3207–3212.
Fedtke, I., Gotz, F., Peschel, A., 2004. Int. J. Med. Microbiol. 294, 189–194.
Foster, J.S., Kolenbrander, P.E., 2004. Appl. Environ. Microbiol. 70, 4340–4348.
Freitas, L.B., Vassilakos, N., Arnebrant, T., 1993. J. Periodontics Res. 28, 92–97.
Gjermo, P., 1989. J. Dent. Res. 68, 1602–1608.
Haps, S., Slot, D.E., Berchier, C.E., Van der Weijden, G.A., 2008. Int. J. Dent. Hyg. 6, 290–303.
Heitz-Mayfield, L.J., Mombelli, A., 2014. Int. J. Oral Maxillofac. Implants 29.
Herzberg, M.C., 2000. Oral streptococci in health and disease. In: Stevens, D.L., Kaplan, E.L. (Eds.), Streptococcal Infections: Clinical Aspects, Microbiology, and Molecular Pathogenesis. Oxford University Press, USA, pp. 338–339.
Hussain, M., Northoff, H., Gehring, F.K., 2015. Biosens. Bioelectron. 66, 579–584.
Hussain, M., Rupp, F., Wendel, H.P., Gehring, F.K., 2018. Trends Anal. Chem. 102, 194–209.
Jakubovics, N., Kolenbrander, P., 2010. Oral Dis. 16, 729–739.
Joiner, A., Elofsson, U.M., Arnebrant, T., 2006. Eur. J. Oral Sci. 114, 337–342.
Jones, C.G., 1997. Periodontol 2000 15, 55–62.
Kerrigan, S.W., Cox, D., 2010. Cell Mol. Life Sci. 67, 513–523.
Kozlovsky, A., Artzi, Z., Moses, O., Kamin-Belsky, N., Greenstein, R.B., 2006. J. Periodontol. 77, 1194–1200.
Krajewski, S., Rheinlaender, J., Ries, P., Canjuga, D., Mack, C., Scheideler, L., Schaffer, T.E., Geis-Gerstorfer, J., Wendel, H.P., Rupp, F., 2014. Anal. Bioanal. Chem. 406, 3395–3406.
Lendenmann, U., Grogan, J., Oppenheim, F.G., 2000. Adv. Dent. Res. 14, 22–28.
Marcus, I.M., Herzberg, M., Walker, S.L., Freger, V., 2012. Langmuir 28 (15), 6396–6402.
McCubbin, G.A., Praporski, S., Piantavigna, S., Knappe, D., Hoffmann, R., Bowie, J.H., Separovic, F., Martin, L.L., 2011. Eur. Biophys. J. 40, 437–446.
McNab, R., Forbes, H., Handley, P.S., Loach, D.M., Tannock, G.W., Jenkinson, H.F., 1999. J. Bacteriol. 181, 3087–3095.
Nobbs, A.H., Jenkinson, H.F., Jakubovics, N.S., 2011. J. Dent. Res. 90, 1271–1278.
Olsson, A.L., van der Mei, H.C., Busscher, H.J., Sharma, P.K., 2009. Langmuir 25, 1627–1632.
Olsson, A.L., van der Mei, H.C., Busscher, H.J., Sharma, P.K., 2011. J. Colloid Interface Sci. 357, 135–138.
Pitten FA, K.A., 2001. Arzneim. Forsch./ Drug Res. 51, 588–595.
Pomorska, A., Shchukin, D., Hammond, R., Cooper, M.A., Grundmeier, G., Johannsmann, D., 2010. Anal. Chem. 82, 2237–2242.
Preočanin, T., Kallay, N., 2006. Croat. Chem. Acta 79, 95–106.
Reviakine, I., Johannsmann, D., Richter, R.P., 2011. Anal. Chem. 83, 8838–8848.
Rimondini, L., Fare, S., Brambilla, E., Felloni, A., Consonni, C., Brossa, F., Carrassi, A., 1997. J. Periodontol. 68, 556–562.
Roberts, W.R., Addy, M., 1981. J. Clin. Periodontol. 8, 295–310.
Rolla, G., Melsen, B., 1975. J. Dent. Res. 54, B57–B62 (Spec. No B).
Ruhl, S., Sandberg, A.L., Cisar, J.O., 2004. J. Dent. Res. 83, 505–510.
Rupp, F., Haupt, M., Eichler, M., Doering, C., Klostermann, H., Scheideler, L., Lachmann, S., Oehr, C., Wendel, H.P., Decker, E., Geis-Gerstorfer, J., von Ohle, C., 2012. J. Dent. Res. 91, 104–109.
Sbordone, L., Bortolaia, C., 2003. Clin. Oral Investig. 7, 181–188.
Stewart, P.S., Costerton, J.W., 2001. Lancet 358, 135–138.
Subramani, K., Wismeijer, D., 2012. Int. J. Oral Maxillofac. Implants 27, 1043–1054.
Tacconelli, E., Carrara, E., Savoldi, A., Harbarth, S., Mendelson, M., Monnet, D.L., Pulcini, C., Kahlmeter, G., Kluytmans, J., Carmeli, Y., 2018. Lancet Infect. Dis. 18, 318–327.
Tymchenko, N., Nileback, E., Voinova, M.V., Gold, J., Kasemo, B., Svedhem, S., 2012. Biointerphases 7, 43.
Vitkov, L., Hermann, A., Krautgartner, W., Herrmann, M., Fuchs, K., Klappacher, M., Hannig, M., 2005. Microsc. Res. Tech. 68, 85–89.
Vollmer, W., Blanot, D., de Pedro, M.A., 2008. FEMS Microbiol Rev. 32, 149–167.
Winrow, M.J., 1973. J. Periodontics Res. Suppl. 12, 45–48.
Zitzmann, N.U., Berglundh, T., 2008. J. Clin. Periodontol. 35, 286–291.